Bollettino
Unione Matematica Italiana

Claudio Verdi

Numerical methods for phase transition problems

Bollettino dell'Unione Matematica Italiana, Serie 8, Vol. **1-B** (1998), n.1, p. 83–108.

Unione Matematica Italiana

<http://www.bdim.eu/item?id=BUMI_1998_8_1B_1_83_0>

Bollettino dell'Unione Matematica Italiana, Unione Matematica Italiana, 1998.

Bollettino U. M. I.
(8) **1**-B (1998), 83-108

Numerical Methods for Phase Transition Problems.

CLAUDIO VERDI

Sunto. – *Nel presente articolo si illustrano alcuni dei principali metodi numerici per l'approssimazione di modelli matematici legati ai fenomeni di transizione di fase. Per semplificare e contenere l'esposizione ci siamo limitati a discutere con un certo dettaglio i metodi più recenti, presentandoli nel caso di problemi modello, quali il classico problema di Stefan e l'evoluzione di superficie per curvatura media, solo accennando alle applicazioni e modelli più generali.*

1. – Introduction.

The classical model for phase transitions is the so-called Stefan problem, where the heat equations in the liquid and solid phases are coupled with the Stefan jump condition at the phase change interface. Tracking numerically the free boundary and decoupling the corresponding heat equations presents various difficulties in several space dimensions, that can be avoided using the weak formulation of the Stefan problem in terms of energy density. The interface disappears as an explicit unknown and the ensuing fixed domain methods are very attractive numerically. However the lack of regularity across the free boundary is responsible for global numerical pollution that degrades accuracy for fixed quasi-uniform meshes and constant time-steps. The proper remedy is adaptivity, that is mesh and time-step modification, which makes accurate computations feasible.

We consider first the simplest two-phase Stefan problem in enthalpy form

$$\partial_t u - \Delta\theta = f\,, \quad \theta = \beta(u)\,, \quad \text{in } Q = \Omega \times (0\,,\, T)\,, \tag{1.1}$$

where θ and u are scaled temperature and enthalpy, and the constitutive relation $\beta(s) = \min(s,\, 0) + \max(s - 1,\, 0)$ corresponds to an ideal material with constant thermal properties and unit latent heat. A number of physically justified generalizations of the basic Stefan model describing undercooling and surface tension effects can be considered [83], [85]. They include diffuse interface models, like phase relaxation and phase field systems, Gibbs-Thomson laws, and mean curvature flows.

The finite element analysis of (1.1) with a quasi-uniform mesh of size h and backward finite differences with constant time-step τ was started by Jerome and Rose [41] and is widely reviewed in [54], [80]. An essentially linear rate of conver-

gence $h + \tau$ in two space dimensions for both temperature and energy density in the natural energy spaces was proven recently by Rulla and Walkington [76]. The numerical schemes of [41], [76] provide the best scenario for error analysis, but are difficult to implement and solve because they do not include quadrature. Numerical integration has been extensively studied by Nochetto and Verdi [67], who obtained an optimal rate of convergence $h^{1/2}$ under minimal regularity of data; see also [29], [79]. Linearization and extrapolation methods were analyzed in [51], [68] and [53].

Locally refined meshes for Stefan problems in two space dimensions were first used by Nochetto, Paolini, and Verdi [55], [56]. See also [57]. The adaptive strategy reflects the regularity of the underlying solutions and is based on equidistributing pointwise *a priori* interpolation errors in space and balancing with the truncation errors in time. This is accomplished by extracting information about discrete derivatives as well as by predicting free boundary evolution. A typical triangulation is coarse away from the discrete interface, where meshsize and time-step satisfy a parabolic relation, whereas it is locally refined in the vicinity of the discrete interface for the relation to become hyperbolic. The thickness of the refined region is of order $\tau^{1/2}$ so as to contain the discrete interface for about $\tau^{-1/2}$ time-steps. Mesh changes incorporate an interpolation error which eventually accumulates in time. Its control imposes several constraints on admissible meshes and allowable mesh modifications and leads to the mesh selection algorithm. A new triangulation is completely regenerated upon failure of the mesh admissibility tests; thus consecutive meshes are noncompatible. In turn, an interpolation theory for noncompatible meshes is developed. The proposed adaptive scheme is stable and a rate of convergence of essentially $\tau^{1/2}$ is derived. The main drawback of this methodology is the accurate computation of interface velocity, needed only for *a priori* mesh design, which is rather problematic for degenerate situations and diffuse interfaces.

Recently Nochetto, Schmidt, and Verdi [63], [64], [65] have analyzed and implemented a different approach to mesh and time-step modification, which is based on *a posteriori* error estimates with computable bounds and refinement/coarsening strategies. See also [19]. The adaptive method is stable and convergent upon restricting coarsening. After a localization step in space and time for the estimators to be practical, the adaptive algorithm of [63] equidistributes space discretization errors for a uniform error distribution in time. This strategy leads to optimal meshes, which possess fewer degrees of freedom than those of [55], [56], and requires no estimate of interface velocity nor restrictions in the number of mesh changes.

Mesh adaptation is extremely important also for diffuse interface models in phase transitions. Prototype problems are the phase relaxation model of Visintin [82]

$$\partial_t(\theta + \chi) - \Delta\theta = f\,, \quad \varepsilon_\tau \partial_t \chi + \partial \mathcal{Y}_{[-1,1]}(\chi) \ni \theta\,, \quad \text{in } Q\,, \tag{1.2}$$

and the phase field system of Caginalp [16] based on Landau-Ginzburg theory [1]

$$\partial_t(\theta+\chi)-\Delta\theta=f\,,\quad \varepsilon_\tau\partial_t\chi-\varepsilon_l\Delta\chi+\frac{1}{\varepsilon_l}\chi(\chi^2-1)=\theta\,,\quad \text{in } Q\,. \tag{1.3}$$

Here χ is the phase variable, ε_τ is a time relaxation, ε_l is a lenght scale, and $\partial\mathfrak{Y}_{[-1,1]}$ is the subdifferential of the indicatrix function and acts as a double obstacle. Term $\chi(\chi^2-1)$ in (1.3) could be replaced by a potential with obstacle $\partial\mathfrak{Y}_{[-1,1]}(\chi)-\chi$. Then the phase variable χ ranges between -1 and 1, is constant in most of the domain, and varies abruptly within a narrow transition layer of width of order ε_l. It is worth to mention the application of phase relaxation models to the process of polymer crystalization. Numerous variants of phase field systems, including anisotropic effects, has been considered; it is worth to mention in particular the thermodinamically consistent Penrose-Fife model [38]. The finite element analysis of (1.2) was started by Verdi and Visintin [81] and extended variously to generalized phase relaxation models in [20], [42], [43], [44]. For the numerical approximation of phase field systems we refer to [13], [46], but adaptivity and rigorous *a posteriori* error analysis are still to be investigated.

Surface tension effects with kinetic undercooling can be described by the Stefan model with the Gibbs-Thomson law at the phase transition interface

$$\theta=-\sigma_\kappa\kappa+\sigma_V V\quad \text{on } \Sigma\,. \tag{1.4}$$

Here σ_κ is the surface tension, κ is the sum of the principal curvatures of $\Sigma(t)$ (positive for a convex solid phase $I(t)$), σ_V is a dynamic coefficient, and V is the normal velocity of $\Sigma(t)$ (positive for melting). An adaptive finite element method for the Stefan-Gibbs-Thomson model has been implemented by Schmidt [77]. Recently Visintin [83], [84] has modified this law by $\theta=-\sigma_\kappa\kappa+\alpha(V)$, where α is the cut-off function $\alpha(s)=\max(-1,\min(1,\sigma_V s))$, to include phase nucleation and annihilation.

The Gibbs-Thomson law (1.4) is a mean curvature flow for the interface $\Sigma(t)$

$$V=\kappa+g\,, \tag{1.5}$$

where g is a given kinetic term. Since (1.5) possesses an intrinsic geometric interest, we present some results on its numerical approximation and refer to [62] for an overview. The formulation of (1.5) in terms of the Laplace-Beltrami operator [40] is the base for the parametric finite element method introduced by Dziuk [26], [27], [28]. However the onset of singularities and topological changes restrict the applicability of the parametric method to the smooth regime and demand a proper notion of weak solution.

The level set approach of Osher and Sethian [73] represents $\Sigma(t)$ as the zero level set of a continuous function $w(\cdot,t)$, all whose level sets evolve formally in

the inward normal direction ν according to (1.5); thus w solves in the viscosity sense

$$\frac{1}{|\nabla w|}\,\partial_t w - \operatorname{div}\left(\frac{\nabla w}{|\nabla w|}\right) - g = 0 \qquad \text{in } \mathbb{R}^d \times (0, T). \tag{1.6}$$

The set $\Sigma(t) = \{x \in \Omega\colon w(x, t) = 0\}$ defines uniquely the generalized evolution by mean curvature [18], [35] and coincides with (1.5) as far as the classical flow exists. An equivalent definition in terms of De Giorgi's barriers is presented in [9].

Based on De Giorgi's Γ-convergence, the flow $\Sigma(t)$ can be approximated by the zero level set $\Sigma_\varepsilon(t) = \{x \in \Omega\colon \chi_\varepsilon(x, t) = 0\}$ of the solution χ_ε of the singularly perturbed reaction-diffusion equation with double obstacle

$$\varepsilon\partial_t\chi_\varepsilon - \varepsilon\Delta\chi_\varepsilon - \frac{1}{\varepsilon}\,\chi_\varepsilon + \partial\mathcal{Y}_{[-1,\,1]}(\chi_\varepsilon) \ni \frac{\pi}{4}\,g \qquad \text{in } Q\,. \tag{1.7}$$

This equation is also suggested by Landau-Ginzburg theory of phase transitions and has to be compared with the phase field equation in (1.3). The set $\Sigma_\varepsilon(t)$ is known to converge to $\Sigma(t)$ as $\varepsilon \to 0$ provided $\Sigma(t)$ has empty interior [69] (see also [6], [34]). The proof is based on constructing barriers for (1.7) in terms of the signed distance function to suitable level sets of the solution w of (1.6).

Since the solution χ_ε attains the values -1 and 1 outside a thin noncoincidence set $\mathcal{T}_\varepsilon(t)$ of width of order ε, problem (1.7) has to be solved only within $\mathcal{T}_\varepsilon$. This approach thus retains the geometric structure of the original problem (1.5) while being insensitive to singularity formation. Conforming piecewise linear finite elements combined with mass lumping and forward differences are further used to discretize (1.7) in space and time. Since the discrete problem exhibits both the same local structure of (1.7) and finite speed of propagation, it can be efficiently solved and implemented as a dynamic mesh method [61]. This algorithm only triangulates the transition layer and then updates it, after having computed the discrete solution at the current time-step, to advance the evolution. Such a simple but crucial idea results in savings of computing time and memory allocation and shows the potentials to handle stiffs systems, as phase field and Stefan-Gibbs-Thomson models. In addition enhanced singularity resolution can be obtained via a space-time dependent relaxation parameter and locally refined meshes [60]. Convergence and error estimates of discrete interfaces have been proven by Nochetto and Verdi [71], [72].

The evolution law (1.5) does not depend on the orientation of the surface. However in many physical situations formation of patterns are observed that clearly imply the existence of preferred directions; typical examples are dendritic growth and crystal growth. Bellettini and Paolini [10] have studied the anisotropic interface law $V = \phi^\circ(\nu)(\kappa_\phi + g)$. Here ϕ is a strictly convex Finsler metric, ϕ° is the dual metric, and κ_ϕ is the anisotropic curvature. The unit balls of ϕ and ϕ°

are usually referred to as «Wulff shape» and «Frank diagram», respectively. Crystalline curvature is then obtained as a by-product of lack of strict convexity. The dynamic mesh algorithm can be implemented also in the anisotropic setting [74]; we refer to [37] for simulations with nonconvex anisotropies.

2. – Continuous and discrete Stefan problems.

Let $\Omega \subset \mathbb{R}^d$ ($d \geq 1$) be a bounded convex polyhedral domain; set $Q = \Omega \times (0, T)$ for $T > 0$. Let u_0 denote the initial enthalpy, let $\theta_0 = \beta(u_0) \in W_0^{1,\infty}(\Omega)$ be the initial temperature, and let f be sufficiently smooth. The vanishing Dirichlet boundary condition on θ is assumed only for simplicity; thus the free boundary $\Sigma(t) = \{x \in \Omega\colon \theta(x, t) = 0\}$ does not include $\partial\Omega$. Hereafter $\langle \cdot, \cdot \rangle$ stands for either the inner product in $L^2(\Omega)$ or the duality pairing between $H^{-1}(\Omega)$, $H_0^1(\Omega)$ and $\langle\langle \cdot, \cdot \rangle\rangle_l$ denotes the L^2 inner product on a $(d-1)$-dimensional manifold l.

CONTINUOUS PROBLEM. – *Find* u, θ *such that* $\theta \in L^\infty(0, T; H_0^1(\Omega)) \cap H^1(0, T; L^2(\Omega))$, $u \in W^{1,\infty}(0, T; H^{-1}(\Omega))$, $u_{|t=0} = u_0$,

$$\theta(x, t) = \beta(u(x, t)) \text{ a.e. } (x, t) \in Q\,,$$

and for a.e. $t \in (0, T)$ *and all* $\eta \in H_0^1(\Omega)$ *the following equation holds*

$$\langle \partial_t u, \eta \rangle + \langle \nabla\theta, \nabla\eta \rangle = \langle f, \eta \rangle\,. \tag{2.1}$$

Existence and uniqueness for this problem are known [83].

We introduce the fully discrete problem, which combines continuous piecewise linear finite elements and mass lumping in space with backward differences in time. For other time discretization, like linearization or extrapolation, see [54], [80].

We denote by τ_n the time-step at the n-th step t^n and let $t^N \geq T$.

Let $\mathcal{M}^n$ be a uniformly regular partition of Ω into simplices S [21] with mesh-size density h_n and let $\mathcal{B}^n$ be the collection of interior interelement boundaries e of $\mathcal{M}^n$ in Ω; h_S (resp. h_e) stands for the diameter of $S \in \mathcal{M}^n$ (resp. $e \in \mathcal{B}^n$).

Let $\mathbb{V}^n \subset H_0^1(\Omega)$ be the usual space of continuous piecewise linear finite elements over $\mathcal{M}^n$. Let I^n be the usual Lagrange interpolation operator over $\mathbb{V}^n$. The discrete inner product $\langle \cdot, \cdot \rangle^n$ is defined by the vertex quadrature rule [21]

$$\langle \varphi_1, \varphi_2 \rangle^n = \int_\Omega I^n(\varphi_1 \varphi_2)\, dx\,, \qquad \forall \varphi_1, \varphi_2 \in \mathbb{V}^n\,,$$

which leads to mass lumping. Set $\|\varphi\|_n = (\langle \varphi, \varphi \rangle^n)^{1/2}$ for all $\varphi \in \mathbb{V}^n$.

DISCRETE PROBLEM. – *Given* U^{n-1}, $\Theta^{n-1} \in \mathbb{V}^{n-1}$, *then* $\mathcal{M}^{n-1}$ *and* τ_{n-1} *are modified to get* $\mathcal{M}^n$ *and* τ_n *so as suitable local estimators are kept under tolerance, and thereafter* U^n, $\Theta^n = I^n \beta(U^n) \in \mathbb{V}^n$ *computed by*

$$\frac{1}{\tau_n} \langle U^n - I^n U^{n-1}, \varphi \rangle^n + \langle \nabla \Theta^n, \nabla \varphi \rangle = \langle I^n f(\cdot, t^n), \varphi \rangle^n , \qquad \forall \varphi \in \mathbb{V}^n . \tag{2.2}$$

Using mass lumping and enforcing the constitutive relation only at the nodes introduces some consistency errors but amounts to having a monotone problem. Thus (2.2) is easy to implement and solve via an optimized nonlinear SOR [56] or monotone multigrid methods [47].

We now conclude with further notation. The jump J_e^n of $\nabla \Theta^n$ across $e \in \mathcal{B}^n$ is

$$J_e^n = [\![\nabla \Theta^n]\!]_e \cdot \nu_e = (\nabla \Theta^n_{|S_1} - \nabla \Theta^n_{|S_2}) \cdot \nu_e ,$$

which is well defined if the unit normal vector ν_e to e always points from S_2 to S_1. Let U be the piecewise constant extension of $\{U^n\}$ defined by $U(\cdot, 0) = U^0(\cdot)$ and $U(\cdot, t) = U^n(\cdot)$ for all $t^{n-1} < t \leq t^n$ with $n \geq 1$. Let $e_u = u - U$, $e_\theta = \theta - \beta(U)$, and $E = \|e_\theta\|_{L^2(Q)} + \|e_u\|_{L^\infty(0, T; H^{-1}(\Omega))}$ be the errors. The interior residual R^n is

$$R^n(\cdot) = I^n f(\cdot, t^n) - \frac{1}{\tau_n} (U^n(\cdot) - I^n U^{n-1}(\cdot)) .$$

2.1. *Stability and convergence.* Arbitrary mesh changes may lead to convergence to a wrong solution or divergence even for the heat equation [25]. If mesh $\mathcal{M}^n$ is completely regenerated, as in [55], [56], then $\mathcal{M}^n$ and $\mathcal{M}^{n-1}$ are noncompatible and the interpolation process used in (2.2) to transfer information between consecutive meshes incorporates an error over all triangles of $\mathcal{M}^n$. Time accumulation of this error imposes several restrictions to mesh modification in order to preserve stability and convergence of the discrete scheme (2.2). In [55] the number of mesh changes was limited and triangles crossed by the free boundary were kept fixed. On the other hand if $\mathcal{M}^n$ is obtained from $\mathcal{M}^{n-1}$ by refining/coarsening, and thus $\mathcal{M}^n$ and $\mathcal{M}^{n-1}$ are compatible, the only loss of information between $\mathcal{M}^{n-1}$ and $\mathcal{M}^n$ is due to coarsening. In [64] it is shown that (2.2) remains stable and convergent if coarsening is restricted, whereas refinement operations are always allowed. Precisely, for all $1 \leq n \leq N$ and an arbitrary constant A, the constraints read

$$\|I^n U^{n-1}\|_n^2 - \|U^{n-1}\|_{n-1}^2 \leq \tau_{n-1} \|\nabla \Theta^{n-1}\|_{L^2(\Omega)}^2 , \tag{2.3}$$

$$\|U^{n-1} - I^n U^{n-1}\|_{H^{-1}(\Omega)} \leq \tau_{n-1} A \|h_{n-1} \nabla \Theta^{n-1}\|_{L^2(\Omega)} . \tag{2.4}$$

The constraint (2.3) accounts for the increase in time of the L_x^2 energy due to mesh coarsening and is required for weak stability, whereas (2.4) is required for convergence and limits coarsening in H_x^{-1}. Since I^n does not superconverge in

H_x^{-1}, (2.4) imposes a restriction on the number of mesh coarsenings reminiscent of the mesh constraints in [55], [56]. Both constraints can be imposed locally on each element $S \in \mathcal{M}^n$ and thus can be checked in practice.

Assuming that $\mathcal{M}^n$ is acute (weakly acute in two space dimensions), then (2.3) guarantees the weak stability of the discrete scheme (2.2) [64]

$$\frac{1}{2} \max_{1 \leq n \leq N} \|U^n\|_n^2 + \sum_{n=1}^{N} \|U^n - I^n U^{n-1}\|_n^2 + \sum_{n=1}^{N} \tau_n \|\nabla \Theta^n\|_{L^2(\Omega)}^2 \leq C \,. \tag{2.5}$$

To prove (2.5) we take $\varphi = \tau_n U^n \in \mathbb{V}^n$ in (2.2) and add over n. Since

$$2 \sum_{n=1}^{N} \langle U^n - I^n U^{n-1}, U^n \rangle^n = \|U^N\|_N^2 - \|U^0\|_0^2 + \sum_{n=1}^{N} \|U^n - I^n U^{n-1}\|_n^2 + \sum_{n=1}^{N} (\|U^{n-1}\|_{n-1}^2 - \|I^n U^{n-1}\|_n^2) \,,$$

the effect of mesh modification is apparent in the last term, which incorporates the interpolation error and comes under control via (2.3).

If in addition (2.4) is imposed then, for C independent of T and $H_n = \max_{x \in \Omega} h_n$, the following error estimate holds [64]

$$E \leq C T^{1/2} \max_{1 \leq n \leq N} \left(\tau_n + H_n + T^{1/2} \frac{H_n^2}{\tau_n} \right). \tag{2.6}$$

The proof of (2.6) is based upon taking the difference between the time-discrete form of (2.1) and (2.2) and selecting the test function $\eta = G(u(\cdot, t^n) - U^n) = G e_u^n$, where G is the Green operator. The usual choice for $\varphi \in \mathbb{V}^n$ is a discrete Green's operator G^n, that produces the main effect $\langle \nabla \Theta^n, \nabla (G e_u^n - G^n e_u^n) \rangle = 0$. Cancellation of this term comes at the expense of dealing with the global character of G^n. A different choice for φ, that complicates this term but leads to local estimates and deals with minimal regularity of η, is the Clément interpolation operator Π^n. It satisfies, for all $\eta \in H^k(\Omega)$ and $k = 1, 2$,

$$\begin{cases} \|\eta - \Pi^n \eta\|_{L^2(S)} + h_S \|\nabla(\eta - \Pi^n \eta)\|_{L^2(S)} \leq \tilde{C} h_S^k \, |\eta|_{H^k(\tilde{S})} \,, \\ \|\eta - \Pi^n \eta\|_{L^2(e)} \leq \tilde{C} h_e^{k-1/2} \, |\eta|_{H^k(\tilde{S})} \,, \end{cases} \tag{2.7}$$

where $\tilde{S}$ is the union of all elements surrounding $S \in \mathcal{M}^n$ or $e \in \mathcal{B}^n$ [22]. Constants $\tilde{C}$ depend solely on the minimum angle of the mesh $\mathcal{M}^n$. An important by-product of uniform mesh regularity is that the number of adjacent simplices to a given element is bounded by a constant independent of n, meshsizes, and time-steps.

From (2.6) we infer that if $H_n = o(\tau_n^{1/2})$, which allows for highly graded meshes, the discrete scheme (2.2) with variable meshes and time-steps converges.

Moreover if $H_n = O(\tau_n)$ then the following error estimate is valid

$$E \leq C \max(T, T^{1/2}) \max_{1 \leq n \leq N} H_n .$$

This result extends the error analysis of [67], thereby incorporating mesh and time-step changes, but does not take full advantage of the underlying structure of the Stefan problem. Such a structure is hidden into (2.6) and is exploited in [64].

2.2. *A posteriori error estimates.* We first represent the error E for any numerical method in terms of parabolic residuals and next exploit Galerkin orthogonality to express the finite element residuals in terms of computable quantities. A detailed proof of the rigorous *a posteriori* error estimates can be found in [63].

2.2.1. Error representation formula. The discrete solution U of (1.1) satisfies

$$\partial_t U - \Delta\beta(U) = f - \mathcal{R} \quad \text{in } Q , \tag{2.8}$$

where the parabolic residual $\mathcal{R}$ is a distribution with singular components and oscillatory behavior; thus it should be measured in negative norms that quantify oscillations better. We subtract (2.8) from (1.1) and integrate by parts over Q against a smooth test function ζ vanishing on $\partial\Omega \times (0, T)$. The error e_u satisfies

$$\langle e_u, \zeta\rangle_{|t=T} - \int_0^T \langle e_u, \partial_t \zeta + b\Delta\zeta\rangle = \langle e_u, \zeta\rangle_{|t=0} + \mathcal{R}(\zeta), \tag{2.9}$$

where $0 \leq b(x, t) \leq 1$ is the vanishing discontinuous function

$$b(x, t) = \frac{\beta(u(x, t)) - \beta(U(x, t))}{u(x, t) - U(x, t)} \quad \text{if } u(x, t) \neq U(x, t), \quad b(x, t) = 1 \text{ otherwise},$$

and the parabolic residual $\mathcal{R}(\zeta)$ is the distribution

$$\mathcal{R}(\zeta) = \langle U, \zeta\rangle_{|t=0} - \langle U, \zeta\rangle_{|t=T} + \int_Q (f\zeta + U\partial_t \zeta + \beta(U)\,\Delta\zeta) . \tag{2.10}$$

We can represent the error E in terms of $\mathcal{R}(\zeta)$ if $\zeta(\cdot, T)$ and $\partial_t \zeta + b\Delta\zeta$ in (2.9) comes from the backward parabolic problems with operator in nondivergence form

$$\partial_t \psi + (b + \delta)\,\Delta\psi = -b^{1/2}\chi \quad \text{in } Q , \qquad \psi(\cdot, T) = 0 \quad \text{in } \Omega , \tag{2.11}$$

$$\partial_t \phi + (b + \delta)\,\Delta\phi = 0 \quad \text{in } Q , \qquad \phi(\cdot, T) = \varrho \quad \text{in } \Omega , \tag{2.12}$$

where $\delta > 0$ is a regularization parameter to be chosen later, ψ, $\phi = 0$ on $\partial\Omega \times (0, T)$, and $\chi \in L^2(Q)$, $\varrho \in H_0^1(\Omega)$ [48]. Evaluation of $\mathcal{R}(\zeta)$ depends on regularity of ζ which, in turn, dictates the weights (powers of meshsize and time-step) of the *a posteriori* error estimators of § 2.3. In contrast to the heat equation, problems (2.11) and (2.12) do not exhibit any regularizing effect and are not computable in that b is discontinuous and depends on both u and U. It is easy to check that [52], [63]

$$2 \sup_{0 \le t \le T} \|\nabla\psi(\cdot, t)\|^2_{L^2(\Omega)}, \frac{1}{1+\delta} \|\partial_t \psi\|^2_{L^2(Q)}, 4\delta \int_0^T |\psi|^2_{H^2(\Omega)} \le \|\chi\|^2_{L^2(Q)}, \tag{2.13}$$

$$\sup_{0 \le t \le T} \|\nabla\phi(\cdot, t)\|^2_{L^2(\Omega)}, \frac{2}{1+\delta} \|\partial_t \phi\|^2_{L^2(Q)}, 2\delta \int_0^T |\phi|^2_{H^2(\Omega)} \le \|\nabla\varrho\|^2_{L^2(\Omega)}. \tag{2.14}$$

We define the negative norms of the residuals $\mathcal{R}(\psi)$ and $\mathcal{R}(\phi)$ for $k = 1, 2$,

$$\Psi_{-k} = \sup_{\chi \in L^2(Q)} \frac{|\mathcal{R}(\psi)|}{\|D^{(k)}\psi\|_{L^2(Q)}}, \qquad \Phi_{-k} = \sup_{\varrho \in H_0^1(\Omega)} \frac{|\mathcal{R}(\phi)|}{\|D^{(k)}\phi\|_{L^2(Q)}},$$

and set $R_{-1} = \Psi_{-1} + \Phi_{-1}$, $R_{-2} = \Psi_{-2} + (1/\sqrt{2})\,\Phi_{-2}$, and $a = 1 + 1/\sqrt{2}$. On using that

$$\psi(\cdot, T) = 0, \qquad -\int_0^T \langle e_u, \partial_t\psi + b\Delta\psi\rangle = \langle e_u, b^{1/2}\chi\rangle + \delta\langle e_u, \Delta\psi\rangle,$$

$$\phi(\cdot, T) = \varrho, \qquad -\int_0^T \langle e_u, \partial_t\phi + b\Delta\phi\rangle = \delta\langle e_u, \Delta\phi\rangle,$$

and that $e_u b^{1/2} = (e_u e_\theta)^{1/2} \ge |e_\theta|$, $|e_u| \le 1 + |e_\theta|$, from (2.9) we get alternatively

$$\left(1 - \frac{a}{\sqrt{2}}\,\delta^{1/2}\right) \|e_\theta\|_{L^2(Q)} + \|e_u(\cdot, T)\|_{H^{-1}(\Omega)} \le a\|e_u^0\|_{H^{-1}(\Omega)} + R_{-1} + \frac{a}{\sqrt{2}}\,|Q|^{1/2}\,\delta^{1/2},$$

$$(2 - a\delta^{1/2})\,\|e_\theta\|_{L^2(Q)} + \|e_u(\cdot, T)\|_{H^{-1}(\Omega)} \le \sqrt{2}\,a\|e_u^0\|_{H^{-1}(\Omega)} + R_{-2}\,\delta^{-1/2} + a|Q|^{1/2}\delta^{1/2}.$$

The first estimate uses only first space derivatives of ψ and ϕ, whereas the second one exploits the additional, but nonuniform in δ, H^2 space regularity of ψ and ϕ. Either sending $\delta \to 0$ or optimizing δ with $\delta_0 = R_{-2}/a|Q|^{1/2}$, we obtain the two representation formulae valid for any numerical method (Approaches I

and II)

$$E \leq a\|e_u^0\|_{H^{-1}(\Omega)} + R_{-1}\,, \tag{2.15}$$

$$E \leq \sqrt{2}\,a\|e_u^0\|_{H^{-1}(\Omega)} + 2\begin{cases} (a|Q|^{1/2}R_{-2})^{1/2} & \text{if } a^2\delta_0 \leq 1\,, \\ aR_{-2} & \text{if } a^2\delta_0 > 1\,. \end{cases} \tag{2.16}$$

We expect δ_0 to be small, and thus Approach II to work best, because it involves $\mathcal{R}(\psi)$ and $\mathcal{R}(\phi)$; however this cannot be guaranteed *a priori*.

2.2.2. *A posteriori* error estimates. Integrating (2.10) by parts, $\mathcal{R}(\zeta)$ becomes

$$\begin{aligned} \mathcal{R}(\zeta) = {} & \sum_{n=1}^{N} \int_{t^{n-1}}^{t^n} (\langle R^n, \zeta\rangle - \langle \nabla\beta(U^n), \nabla\zeta\rangle) + \\ & \sum_{n=1}^{N} \langle U^{n-1} - I^n U^{n-1}, \zeta(\cdot, t^{n-1})\rangle + \\ & \sum_{n=1}^{N} \int_{t^{n-1}}^{t^n} \frac{1}{\tau_n} \langle U^n - I^n U^{n-1}, \zeta - \zeta(\cdot, t^{n-1})\rangle + \\ & \sum_{n=1}^{N} \int_{t^{n-1}}^{t^n} \langle f - I^n f(\cdot, t^n), \zeta\rangle\,. \end{aligned} \tag{2.17}$$

We next use Galerkin orthogonality, that is we rewrite the discrete problem (2.2) as

$$\langle R^n, \varphi\rangle - \langle \nabla\beta(U^n), \nabla\varphi\rangle = \text{consistency terms} \qquad \forall \varphi \in \mathbb{V}^n\,, \tag{2.18}$$

where c.t. $= (\langle R^n, \varphi\rangle - \langle R^n, \varphi\rangle^n) + \langle \nabla(I^n\beta(U^n) - \beta(U^n)), \nabla\varphi\rangle$. Note that c.t. would be 0 without variational crimes (mass lumping and lumped constitutive relation). Upon subtracting (2.18) from the right hand side of (2.17) we arrive at

$$\begin{aligned} \mathcal{R}(\zeta) = {} & \sum_{n=1}^{N} \int_{t^{n-1}}^{t^n} (\langle R^n, \zeta - \varphi\rangle - \langle \nabla I^n\beta(U^n), \nabla(\zeta - \varphi)\rangle) + \\ & \sum_{n=1}^{N} \langle U^{n-1} - I^n U^{n-1}, \zeta(\cdot, t^{n-1})\rangle + \\ & \sum_{n=1}^{N} \int_{t^{n-1}}^{t^n} \frac{1}{\tau_n} \langle U^n - I^n U^{n-1}, \zeta - \zeta(\cdot, t^{n-1})\rangle + \text{c.t.}\,. \end{aligned}$$

We now estimate each term I to IV separately and argue with $\zeta = \psi$ solution of (2.11). We decompose the integral $\langle \nabla \Theta^n, \nabla(\psi - \varphi)\rangle$ over all elements $S \in \mathcal{M}^n$

$$-\langle \nabla I^n \beta(U^n), \nabla(\psi - \varphi)\rangle = \sum_{e \in \mathcal{B}^n} \langle\!\langle J_e^n, \psi - \varphi \rangle\!\rangle_e \qquad \forall \varphi \in \mathbb{V}^n .$$

Selecting $\varphi(\cdot, t) = \Pi^n \psi(\cdot, t)$ for $t^{n-1} < t \leqslant t^n$ and using (2.7) and H_x^1 regularity of ψ, we get (Approach I)

$$|\mathrm{I}| \leqslant C_1 \sum_{n=1}^{N} \int_{t^{n-1}}^{t^n} \left(\sum_{S \in \mathcal{M}^n} h_S^2 \|R^n\|_{L^2(S)}^2 \right)^{1/2} \|\nabla \psi(\cdot, t)\|_{L^2(\Omega)} ,$$

$$|\mathrm{II}| \leqslant C_2 \sum_{n=1}^{N} \int_{t^{n-1}}^{t^n} \left(\sum_{e \in \mathcal{B}^n} h_e \|J_e^n\|_{L^2(e)}^2 \right)^{1/2} \|\nabla \psi(\cdot, t)\|_{L^2(\Omega)} .$$

Alternatively, on using H_x^2 regularity of ψ, we can also write (Approach II)

$$|\mathrm{I}| \leqslant C_1 \sum_{n=1}^{N} \int_{t^{n-1}}^{t^n} \left(\sum_{S \in \mathcal{M}^n} h_S^4 \|R^n\|_{L^2(S)}^2 \right)^{1/2} |\psi(\cdot, t)|_{H^2(\Omega)} ,$$

$$|\mathrm{II}| \leqslant C_2 \sum_{n=1}^{N} \int_{t^{n-1}}^{t^n} \left(\sum_{e \in \mathcal{B}^n} h_e^3 \|J_e^n\|_{L^2(e)}^2 \right)^{1/2} |\psi(\cdot, t)|_{H^2(\Omega)} .$$

Term III is simply bounded via $H^{-1}(\Omega) - H_0^1(\Omega)$ duality and

$$|\mathrm{IV}| \leqslant \left(\sum_{n=1}^{N} \tau_n \|U^n - I^n U^{n-1}\|_{L^2(\Omega)}^2 \right)^{1/2} \left(\int_0^T \|\partial_t \psi\|_{L^2(\Omega)}^2 \right)^{1/2} .$$

Similar estimates are valid for $\zeta = \phi$ solution of (2.12). Neglecting the consistency terms just for simplicity and using the *a priori* extimates (2.13) and (2.14), we get the following bounds for the residuals $\mathcal{R}(\psi)$ and $\mathcal{R}(\phi)$

$$\frac{|\mathcal{R}(\psi)|}{\|\chi\|_{L^2(Q)}} \leqslant \frac{1}{\sqrt{2}}\, \mathcal{E}_3 + (1+\delta)^{1/2}\, \mathcal{E}_4 + \begin{cases} (\mathcal{E}_1^{\mathrm{I}} + \mathcal{E}_2^{\mathrm{I}})/\sqrt{2} , \\ \delta^{-1/2} (\mathcal{E}_1^{\mathrm{II}} + \mathcal{E}_2^{\mathrm{II}})/2 , \end{cases}$$

$$\frac{|\mathcal{R}(\phi)|}{\|\nabla \varrho\|_{L^2(\Omega)}} \leqslant \mathcal{E}_3 + \frac{1}{\sqrt{2}}\, (1+\delta)^{1/2}\, \mathcal{E}_4 + \begin{cases} \mathcal{E}_1^{\mathrm{I}} + \mathcal{E}_2^{\mathrm{I}} , \\ \delta^{-1/2} (\mathcal{E}_1^{\mathrm{II}} + \mathcal{E}_2^{\mathrm{II}})/\sqrt{2} , \end{cases}$$

where the error indicators for Approach I are given by

$$\mathcal{E}_1^{\mathrm{I}} = C_1 \sum_{n=1}^{N} \tau_n \Big(\sum_{S \in \mathcal{R}^n} h_S^2 \|R^n\|_{L^2(S)}^2 \Big)^{1/2} \qquad \text{interior residual},$$

$$\mathcal{E}_2^{\mathrm{I}} = C_2 \sum_{n=1}^{N} \tau_n \Big(\sum_{e \in \mathcal{B}^n} h_e \|J_e^n\|_{L^2(e)}^2 \Big)^{1/2} \qquad \text{jump residual},$$

$$\mathcal{E}_3 = \sum_{n=1}^{N} \|U^{n-1} - I^n U^{n-1}\|_{H^{-1}(\Omega)} \qquad \text{coarsening},$$

$$\mathcal{E}_4 = \Big(\sum_{n=1}^{N} \tau_n \|U^n - I^n U^{n-1}\|_{L^2(\Omega)}^2 \Big)^{1/2} \qquad \text{time residual},$$

and for Approach II by

$$\mathcal{E}_1^{\mathrm{II}} = C_1 \Big(\sum_{n=1}^{N} \tau_n \sum_{S \in \mathcal{R}^n} h_S^4 \|R^n\|_{L^2(S)}^2 \Big)^{1/2} \qquad \text{interior residual},$$

$$\mathcal{E}_2^{\mathrm{II}} = C_2 \Big(\sum_{n=1}^{N} \tau_n \sum_{e \in \mathcal{B}^n} h_e^3 \|J_e^n\|_{L^2(e)}^2 \Big)^{1/2} \qquad \text{jump residual}.$$

Setting $\mathcal{E}_0 = \|u_0 - U^0\|_{H^{-1}(\Omega)}$ (initial error), we can argue as in deriving (2.15) and (2.16) and conclude with the *a posteriori* error estimates for Approaches I and II

$$\|e_\theta\|_{L^2(Q)} + \|e_u\|_{L^\infty(0,\,T;\,H^{-1}(\Omega))} \leq \mathcal{E}^{\mathrm{k}}(u_0, f,\, T,\, \Omega;\, U,\, h,\, \tau), \tag{2.19}$$

where

$$\mathcal{E}^{\mathrm{I}} = a(\mathcal{E}_0 + \mathcal{E}_1^{\mathrm{I}} + \mathcal{E}_2^{\mathrm{I}} + \mathcal{E}_3 + \mathcal{E}_4),$$

$$\mathcal{E}^{\mathrm{II}} = \sqrt{2}\, a(\mathcal{E}_0 + \mathcal{E}_3) + 3a\mathcal{E}_4 + 2a \begin{cases} |Q|^{1/4} (\mathcal{E}_1^{\mathrm{II}} + \mathcal{E}_2^{\mathrm{II}})^{1/2} & \text{if } a^2(\mathcal{E}_1^{\mathrm{II}} + \mathcal{E}_2^{\mathrm{II}}) \leq |Q|^{1/2}, \\ a(\mathcal{E}_1^{\mathrm{II}} + \mathcal{E}_2^{\mathrm{II}}) & \text{if } a^2(\mathcal{E}_1^{\mathrm{II}} + \mathcal{E}_2^{\mathrm{II}}) > |Q|^{1/2}. \end{cases}$$

The indicators $\mathcal{E}^{\mathrm{k}}$ can be evaluated explicitly in terms of the computed solution U, initial datum u_0, and source term f. They are essential and are also present for the heat equation, but with different weights and cumulative effect in time [33], thereby reflecting the degenerate nature of (1.1). The indicators associated to the consistency terms are not essential and could in principle be removed at the expense of complicating the implementation of (2.2).

It is not obvious that $\mathcal{E}^{\mathrm{k}} \to 0$ and so $E \to 0$ as $h,\ \tau \to 0$, because $\mathcal{E}^{\mathrm{k}}$ in (2.19) depends on discrete quantities that change with h and τ. On the other hand, the stability and error analysis of § 2.1 demonstrate that this goal is achievable. Convergence of the adaptive algorithm remains a challenging open problem.

2.3. *Adaptive algorithm and simulation.* Since the error estimators $\mathcal{E}^k$ in (2.19) entail an L^1 or L^2 accumulation in time, they are impractical in that the entire evolution history would be needed to control the error. In [63], [65] we overcome this hurdle upon equidistributing the errors in time in the L^∞ norm and optimizing the error distribution in space at each time-step. Let $E_0(S)$ denote the initial error and $E_h^n(S)$ the spatial error at the element $S \in \mathcal{M}^n$ and let E_τ^n denote the time residual. Let $M^n = \operatorname{card} \mathcal{M}^n$. Given an error tolerance ε, refinement Γ and coarsening γ parameters satisfying $\Gamma_0 + \Gamma_\tau + \Gamma_h \leq 1$, $\gamma_\tau < \Gamma_\tau$, $\gamma_h < \Gamma_h$, for Approach I the adaptive algorithm selects time-steps and mesh densities as follows. Starting with $\tau_n = \tau_{n-1}$, the algorithm checks whether $E_\tau^n > \Gamma_\tau \varepsilon$ or $E_\tau^n < \gamma_\tau \varepsilon$. In the first case τ_n is reduced, whereas in the second one (corresponding to τ_n being too small) τ_n is accepted but the initial guess for the next time-step size is enlarged. Next, starting from $\mathcal{M}^n = \mathcal{M}^{n-1}$, for any $S \in \mathcal{M}^n$ the algorithm checks whether $M^n E_h^n(S) > \Gamma_h^2 \varepsilon^2$ or $M^n E_h^n(S) < \gamma_h^2 \varepsilon^2$. Then refinement and coarsening operations are performed accordingly, with the precaution of choosing $\gamma_h \ll \Gamma_h$ properly to prevent from alternating such operations over the same elements. The initial mesh is created from a coarse mesh $\mathcal{M}^0$ upon bisecting all $S \in \mathcal{M}^0$ such that $M^0 E_0(S) > \Gamma_0^2 \varepsilon^2$. Elements are either refined or coarsened via «bisection» [15].

EXAMPLE. – We conclude this section with an intriguing example with persistent corner singularity for a one-phase Stefan problem in two space dimensions, for which the use of adaptive local refinements has been essential. The key question, posed by Athanasopoulos, Caffarelli, and Salsa [5], is whether or not $\pi/2$ is the critical angle beyond which the interface immediately regularizes. The simulations in [66] seem to indicate that the critical angle is actually larger than $\pi/2$.

Let $\Omega = (-0.1, 0.1)^2$, $T = 0.1$, and $g(t) = 2.1 - 10t$. The function

$$u^+(\varrho, \omega, t) = \varrho^{g(t)} \cos(\omega g(t)) \quad \text{if } g(t)\,|\omega| < \frac{\pi}{2}, \qquad u^+ = 0 \quad \text{otherwise},$$

in polar coordinates (ϱ, ω), is a supersolution provided $2g^3(t)\,\varrho^{g(t)-2} + \pi g'(t) \leq 0$. This can only be enforced for $g(t) > 2$ in a shrinking domain as $g(t) \downarrow 2$, and provides some support to the above conjecture that the opening $\pi/2$, and thus $\omega_0 = \pi/4$, could be critical. Function u^+ is only used to set up initial and boundary conditions for the simulations, with an angle shift $\omega - 0.2$ to avoid grid orientation effects.

Figure 2.1 displays the interfaces and zooms with scaling factors 1, 4, 16, 64 for a quite accurate run with $\varepsilon = 1$. The solution shows a corner at the origin which persists for some time, while the angle widens. The corner seems to regularize when the angle is already larger than $\pi/2$. Figure 2.2 contains a representative locally refined mesh and zoom with scaling factor 16. It is clear that the interface is correctly captured by the algorithm even though the solution is very

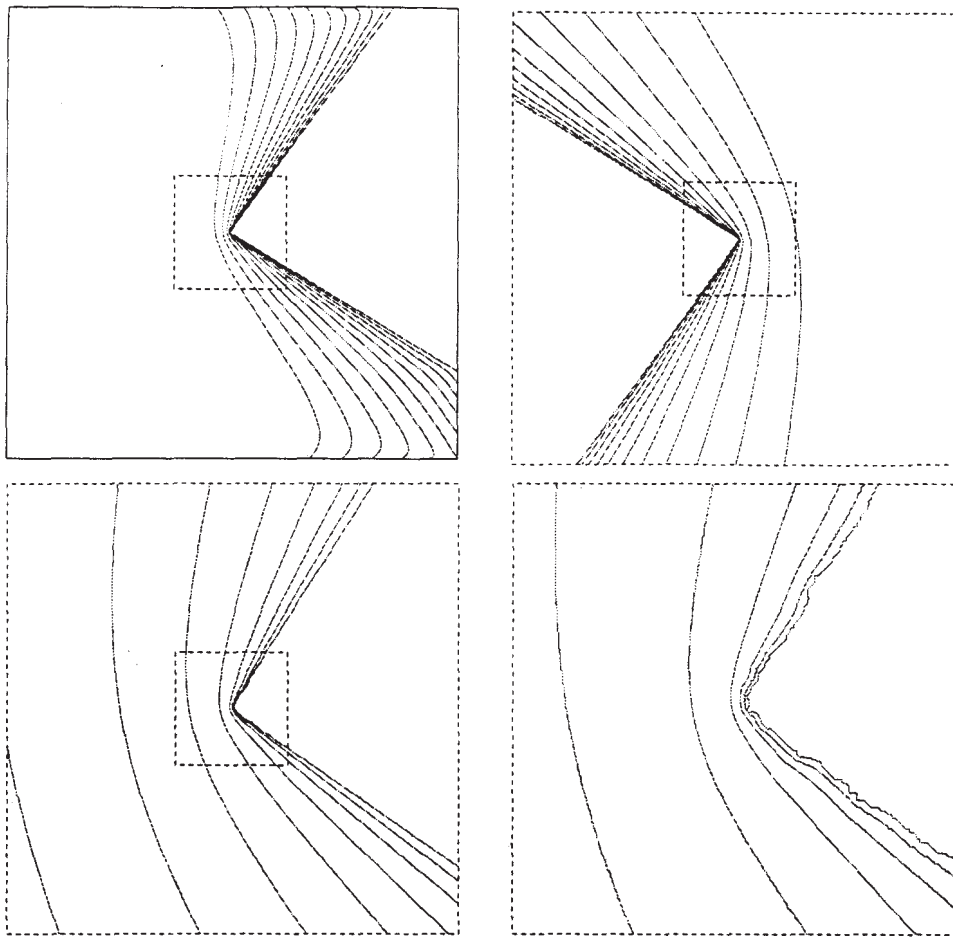

Fig. 2.1 – Zoom of interfaces with scaling factors 1, 4, 16, 64 for tolerance $\varepsilon = 1$, at times $t = 0.01\ k$, $0 \leq k \leq 10$ (top) resp. $3 \leq k \leq 10$ (bottom).

degenerate near the origin. We stress that the minimum value of the meshsize is 1.2×10^{-5}, which would require 10^8 triangles in Ω for a fixed quasi-uniform mesh to capture the singularity: adaptivity and local mesh refinement are thus essential.

The stationary corner singularity above is a hyperbolic effect and reveals that the Stefan problem possesses a hyperbolic behavior near the interface. This is a structural property already used in [55], [56] for *a priori* design of locally refined meshes and a consequence of the *a posteriori* mesh design of [65], [66].

2.4. *Stefan problem with surface tension.* Let the free boundary $\Sigma(t)$ be parametrized by local charts $\Phi_i(t)$: $\mathcal{S}_i \to \mathbb{R}^d$, $i \in I$, with parameter domains $\mathcal{S}_i \subset \mathbb{R}^{d-1}$ independent of t and let Δ denote the Laplace-Beltrami operator on

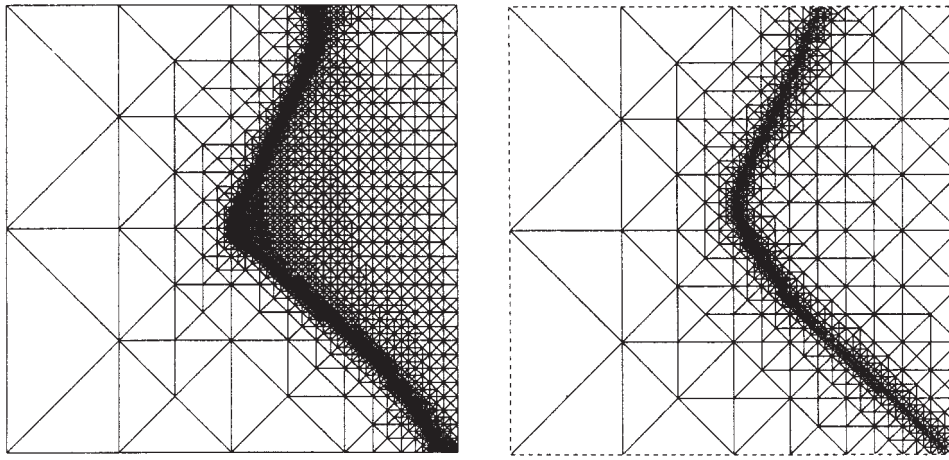

Fig. 2.2 – Mesh and zoom with scaling factor 16 for tolerance $\varepsilon = 4$, at time $t = 0.06$ (number of triangles $M = 15,273$).

$\Sigma(t)$. Upon integrating the heat equations by parts over Ω against a test function $\eta \in H_0^1(\Omega)$ and using Stefan and Gibbs-Thomson laws, the solution θ, Σ of the Stefan problem with surface tension and kinetic unsercooling satisfies [17], [77]

$$\langle \partial_t \theta, \eta \rangle + \langle \nabla\theta, \nabla\eta \rangle + \Big\langle\!\Big\langle \frac{1}{\sigma_V}\,\theta, \eta \Big\rangle\!\Big\rangle_{\Sigma(t)} + \Big\langle\!\Big\langle \frac{\sigma_\kappa}{\sigma_V}\,\kappa, \eta \Big\rangle\!\Big\rangle_{\Sigma(t)} = 0 \qquad \forall \eta \in H_0^1(\Omega), \tag{2.20}$$

$$\frac{\sigma_V}{\sigma_\kappa}\,\partial_t \Phi_i - \underline{\Delta}\Phi_i = \left(\frac{1}{\sigma_\kappa}\,\theta\nu\right) \circ \Phi_i \qquad \text{in } \mathcal{S}_i \times (0,T), \quad i \in I\,. \tag{2.21}$$

An adaptive finite element algorithm for (2.20), (2.21) based on Dziuk's parametric finite element method for mean curvature flow [26] and a heat equation solver has been implemented by Schmidt [77]. The nonlinear system (2.20), (2.21) is converted into a sequence of decoupled linear equations via a semi-implicit time discretization. Using a global parametrization $\Phi^n \in H^1(\Sigma^{n-1})^d$ of the next manifold Σ^n over the previous one Σ^{n-1}, namely $\Sigma^n = \Phi^n(\Sigma^{n-1})$ with Φ^n independent of the choice of local charts, the semidiscrete problem with $\sigma_V = \sigma_\kappa = 1$ reads

$$\frac{1}{\tau_n}\,\big\langle\!\big\langle \Phi^n - \mathrm{id}_{\Sigma^{n-1}}, \xi \big\rangle\!\big\rangle_{\Sigma^{n-1}} + \big\langle\!\big\langle \underline{\nabla}^{n-1}\Phi^n, \underline{\nabla}^{n-1}\xi \big\rangle\!\big\rangle_{\Sigma^{n-1}} = \big\langle\!\big\langle \theta^{n-1}\nu^{n-1}, \xi \big\rangle\!\big\rangle_{\Sigma^{n-1}}\,, \tag{2.22}$$

$$\frac{1}{\tau_n}\,\langle \theta^n - \theta^{n-1}, \eta \rangle + \langle \nabla\theta^n, \nabla\eta \rangle + \big\langle\!\big\langle \theta^n, \eta \big\rangle\!\big\rangle_{\Sigma^n} = -\big\langle\!\big\langle \kappa^n, \eta \big\rangle\!\big\rangle_{\Sigma^n}\,, \tag{2.23}$$

for all $\xi \in H^1(\Sigma^{n-1})^d$ and $\eta \in H_0^1(\Omega)$. Here $\underline{\nabla}^{n-1}$ denotes the covariant (tangential) derivative on Σ^{n-1}. Given θ^{n-1}, Σ^{n-1}, first (2.22) moves the interface Σ^{n-1}

to the new position Σ^n using θ^{n-1} and the Laplace-Beltrami operator on Σ^{n-1} and next (2.23) computes the new temperature field θ^n using Σ^n and its curvature κ^n. Equations (2.22) and (2.23) are actually discretized by finite elements. To deal with (2.22), a discretization Σ_h^{n-1} of the manifold Σ^{n-1} by a conforming triangular mesh is generated by adapting the previous mesh; the displacement of the grid nodes on the discrete surface obeys to a suitable mesh quality criterium, e.g., it minimizes the difference between the angles around any vertex via a conformal energy. A discretization Σ_h^0 of Σ^0 is based on triangulations of the parameter domains $\mathcal{S}_i$, $i \in I$. The key point for the discretization of (2.23) is the computation of the mean curvature κ_h^n of the piecewise polynomial interface Σ_h^n. To this end a finite element approximation of the identity $\langle\!\langle \kappa^n \nu^n, \xi \rangle\!\rangle_{\Sigma^n} = -\langle\!\langle \underline{\nabla}^n \mathrm{id}_{\Sigma^n}, \underline{\nabla}^n \xi \rangle\!\rangle_{\Sigma^n}$ is used again to define a vector-valued discrete curvature; then the discrete mean curvature κ_h^n is defined as the piecewise linear interpolant against the approximate normals ν_h^n to Σ_h^n. The temperature meshes and the surface meshes are both adaptively generated using the corresponding *a posteriori* estimates but they are not in direct relation. The implementation of the adaptive algorithm in three space dimensions, including anisotropy in the surface tension law, is fully discussed in [77] together with several simulations of dendritic growth.

The Gibbs-Thomson law (1.4) does not account for nucleation or annihilation. Such effects are included in the modified law introduced by Visintin [83], [84] which, with scaled coefficients and cut-off function $\alpha(s) = \max(-1, \min(1, s))$ reads

$$g = -\kappa + \alpha(V). \tag{2.24}$$

Existence of a weak solution of (2.24) in terms of the characteristic function of the evolving set is proven via implicit time discretization; see also [2], [50]. A backward difference approximation of (2.24) with time-step τ is the problem of finding a displaced surface $\Sigma^n = \partial I^n$ having mean curvature $\kappa^n = -g^n + \alpha(-d^{n-1}/\tau)$. Here d^{n-1} stands for the distance from the old surface $\Sigma^{n-1} = \partial I^{n-1}$ that is negative in I^{n-1}. This is equivalent to a prescribed curvature problem which translates into the variational problem $I^n = \operatorname{argmin} \mathcal{A}^n(E)$ of minimizing the surface energy

$$\mathcal{A}^n(E) = \mathcal{P}(E) + \int_E \left(g^n(x) - \alpha(-d^{n-1}(x)/\tau)\right) dx$$

over the sets E of finite perimeter $\mathcal{P}(E)$. The implementation of an adaptive finite element algorithm for (2.24) can be found in [36]. The minimization step is based on a convex minimization algorithm [12]. The numerical approximation of the corresponding modified Stefan model is an interesting applicative problem.

The Stefan problem with surface tension in local thermal equilibrium, that is $\sigma_V = 0$, has been investigated by Luckhaus [49] via a fully implicit time discretization for otherwise instabilities occur. At any time-step the front is moved via minimization of a surface energy involving the new temperature field that, in turn, depends on the latent heat released during phase transition. Numerical simulations via finite differences and a front-tracking algorithm inspired to [11] are given in [3].

3. – Diffuse interfaces and mean curvature flow.

The purely geometric evolution (1.5) exhibits singularities, topological changes such as breaking and merging, extinction, and even nonuniqueness [4], [7]. This restrict the applicability of front-tracking [45] and parametric methods [26] to the smooth regime. Since (1.5) may be viewed as a scaled version of front propagation in phase transitions, where additional energy conservation laws give rise to g, the continuation of the flow past singularities and the design of convergent fully discrete methods insensitive to singularity formation are relevant scientific issues.

3.1. *Level set formulation.* The evolution (1.5) can be defined in a generalized sense, even past singularities, via level set approach [18], [35], [39], [73]. Given a smooth manifold $\Sigma_0 = \partial I_0 \subset \mathbb{R}^d$, let d_0 denote the signed distance function to Σ_0 that is negative in I_0. Let w be the (continuous) viscosity solution of (1.6) with $w(\cdot, 0) = d_0(\cdot)$ [23]. Since $\Sigma(t) = \{x \in \mathbb{R}^d : w(x, t) = 0\}$ is defined uniquely provided $\{x \in \mathbb{R}^d : w(x, 0) = 0\} = \Sigma_0$ and coincides with the classical flow for as long as the latter is smooth, $\Sigma(t)$ defines the generalized evolution (1.5). Let $I(t) = \{x \in \Omega : w(x, t) < 0\}$ and $O(t) = \{x \in \Omega : w(x, t) > 0\}$ be the inside and outside of $\Sigma(t)$. Let Ω be a convex bounded polyhedron on $\mathbb{R}^d$ that contains $\Sigma(t)$ for all $t \leqslant T$. The signed distance function $d(x, t) = \operatorname{dist}(x, I(t)) - \operatorname{dist}(x, O(t))$ satisfies in the viscosity sense [6], [34]

$$\partial_t d(x, t) - \Delta d(x, t) - g(x - d(x, t)\, \nabla d(x, t), t) \geqslant 0 \qquad \text{in } \{d > 0\}. \tag{3.1}$$

We say that $x \in \Sigma(t)$ is a regular point if w is C^1 in a neighborhood of (x, t) and $\nabla w(x, t) \neq 0$; this may occur even past singularities [4]. In any event the level set formulation provides a stable representation of the geometric flow (1.5), in the sense that there exists a Lipschitz constant L such that $\|w\|_{W^{1,1}_\infty(Q)} \leqslant L$. This, in turn, yields a Lipschitz dependence of w under perturbation of data [72]. If w^+ denotes the solution of (1.6) with $w^+(\cdot, 0) = d_0(\cdot) + \pi\alpha$ and $g + \alpha$, then $w \leqslant w^+ \leqslant w + G\alpha$. An immediate consequence is convergence of the perturbed fronts $\Sigma^+(t) = \{x \in \mathbb{R}^d : w^+(x, t) = 0\}$ to $\Sigma(t)$ as $\alpha \to 0$, even past singularities, along

with a linear rate of convergence in a vicinity of regular points $x \in \Sigma(t)$

$$\operatorname{dist}(x, \Sigma^+(t)) \leq C \frac{\|\nabla w(\cdot, 0)\|_{L^\infty(\Omega)}}{|\nabla w(x, t)|} \alpha .$$

In fact, since $w(x + \delta\nu, t) \leq -(1/2)\,\delta |\nabla w(x, t)|$ for δ small and $\nu = -\nabla w(x, t)/|\nabla w(x, t)|$, then $w^+(x + \delta\nu, t) \leq -(1/2)\,\delta |\nabla w(x, t)| + G\alpha = 0$ provided $\delta |\nabla w(x, t)| = 2G\alpha$. Since also $w^+(x, t) \geq w(x, t) = 0$ and w^+ is continuous, we realize that $w^+(\cdot, t)$ has a zero on the straight segment joining $x + \delta\nu$ and x. This result sheds some light on stability properties of the flow (1.5) that make it computable. The idea goes back to [14], and expresses the geometric fact that nondegeneracy together with maximum norm error estimates for solutions lead to interface error control.

A number of applications of the level set approach and corresponding numerical simulations are reviewed in [78].

3.2. *Allen-Cahn approach.* A formulation of (1.5) that is insensitive to singularity formation and very appealing from a numerical viewpoint consists of diffusing the interface $\Sigma(t)$ via a singularly perturbed reaction-diffusion equation [1]. Let $\Psi(s) = 1 - s^2 + \mathfrak{I}_{[-1,1]}(s)$ be a double well potential with obstacles and $c_0 = \int_{-1}^{1} \sqrt{\Psi(s)}\, ds = \pi/2$; another typical example is the quartic $\Psi(s) = (s^2 - 1)^2$. It is known, via De Giorgi's Γ-convergence [24], that the sequence $\{\mathcal{F}_\varepsilon\}_\varepsilon$

$$\mathcal{F}_\varepsilon(\varphi) = \int_{\mathbb{R}^d} \left(\varepsilon |\nabla\varphi|^2 + \frac{1}{\varepsilon} \Psi(\varphi) - c_0 g \varphi \right) dx \qquad \forall \varphi \in H^1(\mathbb{R}^d),$$

Γ-converges to $c_0 \mathcal{F}$, with $\mathcal{F}$ a surface energy functional whose minimizers are characteristic functions $\chi_{\Omega \setminus I}$ corresponding to surfaces ∂I of mean curvature $\kappa = -g$. Since (1.5) is the gradient flow of $\mathcal{F}$, say the fastest way to decrease surface energy, and (1.7) is the gradient flow in L^2 of $\mathcal{F}_\varepsilon$, we can infer that the singular perturbed reaction-diffusion equation (1.7) represents an approximation of the flow (1.5).

3.3. *Convergence analysis.* Let χ_ε be the solution of (1.7) with initial datum $\operatorname{sign} d_0$. The zero level set $\Sigma_\varepsilon(t)$ of $\chi_\varepsilon(\cdot, t)$ is known to converge to $\Sigma(t)$ as $\varepsilon \to 0$ provided $\Sigma(t)$ has empty interior. We present here a formal proof for $g = 0$ and refer to [69] for a rigorous proof in the general case. See also [6], [34] for the quartic potential and [8], [58], [59] for optimal interface error estimates for smooth flows.

Let $\gamma \in C^{1,1}(\mathbb{R})$ be the absolute minimizer of the scaled functional $\mathcal{F}_1$ in one space dimension such that $\gamma(0) = 0$. Thus $\gamma(s) = \sin s$ for $s \in (-\pi/2, \pi/2)$ and

$|\gamma| = 1$ otherwise. The following function is a viscosity supersolution of (1.7)

$$(3.2) \qquad v_\varepsilon^+(x, t) = \gamma(\iota(x, t)), \qquad \iota(x, t) = \frac{d(x, t)}{\varepsilon} - \frac{\pi}{2}, \qquad \forall (x, t) \in Q.$$

Since $v_\varepsilon^+ \geq -1$ and $\gamma''(\iota(x, t))$ is a bounded function, we only have to show that

$$\mathcal{J} v_\varepsilon^+ = \varepsilon \partial_t v_\varepsilon^+ - \varepsilon \Delta v_\varepsilon^+ - \frac{1}{\varepsilon} v_\varepsilon^+ = -\frac{1}{\varepsilon}(\gamma'' + \gamma) + \gamma'(\partial_t d - \Delta d) \geq 0,$$

for $-1 \leq v_\varepsilon^+(x, t) < 1$, that is $\iota(x, t) < \pi/2$. If $\iota < -\pi/2$ then $\gamma = -1$ and $\mathcal{J} v_\varepsilon^+ = 1/\varepsilon > 0$. If $-\pi/2 < \iota < \pi/2$ then $\gamma'' + \gamma = 0$, $\gamma' > 0$, and $d > 0$, whence (3.1) yields $\mathcal{J} v_\varepsilon^+ > 0$.

Now let v_ε^+ be the supersolution defined in (3.2) but in terms of the signed distance function d^+ to $\Sigma^+(t)$, where $\Sigma^+(t)$ is the perturbed flow defined in § 3.1 with $\alpha \geq \varepsilon$. Since $v_\varepsilon^+(\cdot, 0) = \gamma(d^+(\cdot, 0)/\varepsilon - \pi/2) = \gamma(d_0(\cdot)/\varepsilon + \pi/2) \geq \chi_\varepsilon(\cdot, 0)$ in Ω and $v_\varepsilon^+ = \chi_\varepsilon = 1$ on $\partial\Omega \times (0, T)$, then $\chi_\varepsilon \leq v_\varepsilon^+$ in Q and the following convergence results of $\Sigma_\varepsilon(t)$ to $\Sigma(t)$ as $\varepsilon \to 0$, even past singularities, can be easily proven.

For $x \in I(t)$ then $\chi_\varepsilon(x, t) = -1$ for ε small. In fact, if $w(x, t) < 0$ then $w^+(x, t) \leq 0$ and thus $d^+(x, t) \leq 0$ for α small. On using that $\iota^+(x, t) = d^+(x, t)/\varepsilon - \pi/2 \leq -\pi/2$, we deduce $-1 \leq \chi_\varepsilon(x, t) \leq v_\varepsilon^+(x, t) = -1$ for ε small. If $\Sigma(t)$ has empty interior, then this result establishes convergence past singularities of $\Sigma_\varepsilon(t)$ to $\Sigma(t)$ as $\varepsilon \to 0$. Without additional assumptions on $\Sigma(t)$ we cannot expect a rate of convergence.

Let $x \in \Sigma(t)$ be a regular point. Let $\mathrm{thick}(\mathcal{T}_\varepsilon(t); x, \nu)$ denote the thickness of the transition layer $\mathcal{T}_\varepsilon(t) = \{x \in \Omega : |\chi_\varepsilon(x, t)| < 1\}$ in the direction ν at x. For ε small

$$\mathrm{dist}(x, \Sigma_\varepsilon(t)), \quad \mathrm{thick}(\mathcal{T}_\varepsilon(t); x, \nu) \leq C \frac{\|\nabla w(\cdot, 0)\|_{L^\infty(\Omega)}}{|\nabla w(x, t)|} \varepsilon.$$

Let $\alpha = \varepsilon$ so that $w^+(x + \delta\nu, t) \leq 0$ for $\delta |\nabla w(x, t)| = 2G\varepsilon$. Then $\iota^+(x + \delta\nu, t) \leq -\pi/2$, which yields $-1 \leq \chi_\varepsilon(x + \delta\nu, t) \leq v_\varepsilon^+(x + \delta\nu, t) = -1$. Similarly $\chi_\varepsilon(x - \delta\nu, t) = 1$. Then there exists a point on the straight segment connecting $x + \delta\nu$ and $x - \delta\nu$ where $\chi_\varepsilon(\cdot, t)$ vanishes; hence $\mathrm{dist}(x, \Sigma_\varepsilon(t)) \leq \delta$ and $\mathrm{thick}(\mathcal{T}_\varepsilon(t); x, \nu) \leq 2\delta$.

We can simply say that $\Sigma_\varepsilon(t)$ lies between the surfaces $\Sigma^+(t)$ and $\Sigma^-(t)$. Regularity of $\Sigma(t)$ at x is clearly reflected via $|\nabla w(x, t)|^{-1}$, which illustrates how the interface error estimate deteriorates as x moves toward a singularity. It is then the profile of w near a singularity that determines the rate of convergence.

Similar convergence results for the anisotropic Allen-Cahn equation to the anisotropic motion by mean curvature have been proven in [30], [31], [32].

3.4. *Dynamic mesh algorithm.* In contrast to the reaction-diffusion equation with a cubic nonlinearity, the solution $\chi_\varepsilon(\cdot, t)$ of (1.7) varies between the obstacles -1 and 1 within the transition layer $\mathcal{T}_\varepsilon(t)$ and attains the values -1 and 1 elsewhere, irrespective of g. Upon discretizing (1.7) by conforming piecewise linear finite elements combined with mass lumping and forward differences, the discrete problem exhibits both the same local structure of (1.7) and finite speed of propagation.

Let τ be the time-step and let $\mathcal{M}_h$ be a regular partition of Ω into simplices with meshsize h and internal nodes $\{x_i\}_{i=1}^I$. Let $\mathbb{V}_h$ be the space of continuous piecewise linear finite elements over $\mathcal{M}_h$ and $\mathbb{K}_h = \{\varphi \in \mathbb{V}_h\colon |\varphi| \leq 1 \text{ in } \Omega,\ \varphi = 1 \text{ on } \partial\Omega\}$. Let $\langle\cdot, \cdot\rangle_h$ be the usual discrete inner product and let $\boldsymbol{K}$ and $\boldsymbol{M}$ denote the stiffness and lumped mass matrices. The discrete approximation of (1.7) reads as follows.

DISCRETE PROBLEM. – *Set* $X^0 = I_h \gamma(d_0/\varepsilon)$. *For* $1 \leq n \leq N$ *seek* $X^n \in \mathbb{K}_h$ *such that*

$$\frac{\varepsilon}{\tau}\langle X^n - X^{n-1}, \varphi - X^n\rangle_h + \varepsilon\langle \nabla X^{n-1}, \nabla(\varphi - X^n)\rangle - \frac{1}{\varepsilon}\langle X^{n-1}, \varphi - X^n\rangle_h \geq \frac{\pi}{4}\langle g(\cdot, t^n), \varphi - X^n\rangle_h \qquad \forall \varphi \in \mathbb{K}_h\,. \tag{3.3}$$

If we identify any function $\varphi \in \mathbb{K}_h$ with the vector $\{\varphi_i = \varphi(x_i)\}$ of its nodal values, the discrete problem (3.3) equivalently reads

$$\begin{cases} \widetilde{X}_i^n = \left(1 + \dfrac{\tau}{\varepsilon^2}\right) X_i^{n-1} - (\boldsymbol{M}^{-1}\boldsymbol{K}X^{n-1})_i + \dfrac{\tau}{\varepsilon}\,\dfrac{\pi}{4}\, g(x_i, t^n)\,, \\ X_i^n = \max(-1, \min(1, \widetilde{X}_i^n))\,, \qquad \forall 1 \leq i \leq I\,. \end{cases} \tag{3.4}$$

The actual computation of X^n is thus a trivial two-step algebraic process that reduces to a matrix-vector product followed by a componentwise truncation to meet the obstacle constraint. Consequently there is no iteration involved.

The discrete solution exhibits a finite speed of propagation, in the sense that if x_i is a node of $\mathcal{M}_h$ such that $X_j^{n-1} = 1$ for all adjacent nodes x_j to x_i, including x_i, then $X_i^n = X_i^{n-1} = 1$. Hence the discrete transition layer (or noncoincidence set) $\mathcal{T}_h^{n-1}$ cannot enlarge faster than one triangle per time-step and X^n does not have to be computed at vertices lying outside $\overline{\mathcal{T}}_h^{n-1}$. Thus the dynamic implementation of (3.4) only triangulates the transition layer and then updates it, after having solved the discrete problem, to advance the algorithm in time [61]. This dynamic mesh algortihm exhibits the complexity typical of $\mathbb{R}^{d-1}$ without having the drawbacks of front-tracking strategies. In addition, enhanced singularity resolution can be obtained via a space-time dependent relaxation parameter $\varepsilon(x, t) =$

$a(x, t)\varepsilon$ [75]

$$\varepsilon\partial_t(a\chi_\varepsilon) - \varepsilon\nabla\cdot(a\nabla\chi_\varepsilon) - \frac{1}{a\varepsilon}\chi_\varepsilon + \partial\mathfrak{Y}_{[-1,1]}(\chi_\varepsilon) \ni \frac{\pi}{4} \quad \text{in } Q\,.$$

Local transition layer thickness is now expressed in terms of the effective relaxation parameter $a(x, t)\varepsilon$, which is graded towards singularities. The underlying finite element mesh is locally refined according to the mesh density function $ha(x, t)$. Enhanced local accuracy in terms of $a(x, t)\varepsilon$ has been confirmed both numerically and theoretically by rigorous convergence results and error estimates [60], [61], [70].

Discretization and dynamic implementation of the anisotropic reaction-diffusion equation are similar to the isotropic case [74].

3.5. *Convergence analysis for discrete interfaces.* Let $U_{\varepsilon,h,\tau}$, $\Sigma_{\varepsilon,h,\tau}$, and $\mathcal{T}_{\varepsilon,h,\tau}$ indicate the discrete solution and its zero level set and transition region

$$\Sigma_{\varepsilon,h,\tau}(t) = \{x\in\Omega\colon U_{\varepsilon,h,\tau}(x, t) = 0\}\,, \qquad \mathcal{T}_{\varepsilon,h,\tau}(t) = \{x\in\Omega\colon |U_{\varepsilon,h,\tau}(x, t)| < 1\}\,.$$

Convergence and error estimates of both $\Sigma_{\varepsilon,h,\tau}(t)$ and $\mathcal{T}_{\varepsilon,h,\tau}(t)$ to $\Sigma(t)$ past singularities provided $\Sigma(t)$ does not develop interior have been proven by Nochetto and Verdi [71] under various relations among ε, h, and τ. We now discuss briefly the main steps of the discrete convergence analysis, which is based on the construction of discrete barriers. The finite element mesh $\mathcal{M}_h$ over $\Omega\subset\mathbb{R}^2$ is supposed to be quasi-uniform and weakly acute. Under the usual stability condition $\tau\leq C^* h^2$ for explicit time-stepping, the explicit scheme (3.3) satisfies the discrete maximum principle, the key tool for convergence analysis.

Let χ_ε^+ be the solution of (1.7) with $g+\alpha$, $\varepsilon\leq\alpha = o(1)$. Arguing as in § 3.3 and using the perturbed distance d^+, we construct a supersolution v_ε^+ of (1.7), whence

$$\chi_\varepsilon \leq \chi_\varepsilon^+ \leq v_\varepsilon^+ \qquad \text{in } Q\,. \tag{3.5}$$

Let $H_{h,\tau}(\chi_\varepsilon^+)$ denote the approximation of χ_ε^+ obtained via the discrete heat operator with continuous piecewise linear finite elements and mass lumping in space and forward differences in time. If τ, h satisfy the stability constraint $\tau\leq C^* h^2$, the quasi-optimal, up to factors $|\log h|$ and $|\log\varepsilon|$, L^∞ error estimate holds [71]

$$\|\chi_\varepsilon^+ - H_{h,\tau}(\chi_\varepsilon^+)\|_{L^\infty(Q)} \leq Ch\|\chi_\varepsilon^+\|_{C^{0,1;0,1/2}(\overline{Q})} \leq C\frac{h}{\varepsilon}\,. \tag{3.6}$$

The discrete solution $U_{\varepsilon,h,\tau}$ has a prescribed quadratic growth away from $\Sigma_{\varepsilon,h,\tau}$ (discrete nondegeneracy), which for all $(x, t)\in\{-1 < U_{\varepsilon,h,\tau} < -1/2\}$ means

$$\max_{|y-x|\leq r,\ 0\leq t-s\leq r^2} U_{\varepsilon,h,\tau}(y, s) \geq U_{\varepsilon,h,\tau}(x, t) + C\frac{r^2}{\varepsilon^2} > -1 + C\frac{r^2}{\varepsilon^2}\,. \tag{3.7}$$

We combine (3.5) to (3.7) as follows. We first project χ_ε^+ and next lift $H_{h,\tau}(\chi_\varepsilon^+)$ by the small amount $Ch\varepsilon^{-1} \geq \|\chi_\varepsilon^+ - H_{h,\tau}(\chi_\varepsilon^+)\|_{L^\infty(Q)}$ for the resulting function $V_{\varepsilon,h,\tau}^+$ to be a candidate for discrete supersolution. However we must compensate for the antimonotone nature of the potential $-(1/\varepsilon)\chi_\varepsilon$ in (1.7), which gives rise to an error of order $h\varepsilon^{-2}$, and perturb g by the amount $\alpha = Ch\varepsilon^{-2}$. We take $\alpha = o(1)$ and conclude that the parabolic relations τ, $h^2 = o(\varepsilon^4)$ imply that $V_{\varepsilon,h,\tau}^+$ is a discrete supersolution, and thus $V_{\varepsilon,h,\tau}^+ \geq U_{\varepsilon,h,\tau}$. Exploiting the continuous dependence of w with respect to g, this is next used to infer convergence of level sets. In fact, if $x \in I(t)$ then $w^+(x,t) < 0$ for α small, and thus $v_\varepsilon^+ = -1$ in a vicinity of (x,t) results from the explicit construction (3.5). This, in turn, yields

$$U_{\varepsilon,h,\tau} \leq V_{\varepsilon,h,\tau}^+ \leq \chi_\varepsilon^+ + C\frac{h}{\varepsilon} \leq v_\varepsilon^+ + C\frac{h}{\varepsilon} = -1 + C\frac{h}{\varepsilon} < -\frac{1}{2}\,, \tag{3.8}$$

for all $|y-x| \leq r$, $0 \leq t-s \leq r^2$. We finally conclude $U_{\varepsilon,h,\tau}(x,t) = -1$ for otherwise (3.7) and (3.8) would lead to a contradiction for $r^2 \geq Ch\varepsilon$, C large. We would like to point out the importance of dealing with maximum norm estimates for solutions which lead, via nondegeneracy, to convergence of interfaces, the only objects of interest for the geometric problem (1.5). This is a substantially more subtle issue than convergence of solutions [14].

Interface error estimates for regular points $x \in \Sigma(t)$ can be derived using the Lipschitz properties of viscosity solutions of (1.6). For $\alpha = C\varepsilon$ and $\delta|\nabla w(x,t)| = C\varepsilon$ we get $w^+(x+\delta\nu, t) \leq -\varepsilon$. The Lipschitz regularity of w^+ yields $w^+ < 0$, and also $v_\varepsilon^+ = -1$ by (3.5), in an ε-vicinity of $(x+\delta\nu, t)$. Upon arguing as above but with $\alpha = C\varepsilon$, we infer that $U_{\varepsilon,h,\tau}(x+\delta\nu, t) = -1$ and

$$\operatorname{dist}(x, \Sigma_{\varepsilon,h,\tau}(t))\,, \quad \operatorname{thick}(\mathcal{T}_{\varepsilon,h,\tau}(t); x, \nu) \leq C\frac{1}{|\nabla w(x,t)|}\,\varepsilon\,,$$

under the more severe (parabolic) constraints τ, $h^2 = O(\varepsilon^6)$. These ideas are also used to explore how discrete solutions behave near certain singularities, where discrete transition layer thickness becomes of order $\varepsilon^{1/2}$. This quantifies a smearing effect observed in computations [61].

For smooth flows an optimal ε^2 interface rate of convergence is valid provided τ, $h^2 = O(\varepsilon^5)$ and exact integration is used for the linear but rather singular antimonotone term $-(1/\varepsilon)\chi_\varepsilon$ [71].

Convergence of discrete interfaces for the anisotropic curvature flow is a challenging open problem.

REFERENCES

[1] S. M. Allen - J. W. Cahn, *A macroscopic theory for antiphase boundary motion and its application to antiphase domain coarsing,* Acta Metall. Mater., **27** (1979), 1085-1095.

[2] F. ALMGREN - J. E. TAYLOR - L. WANG, *Curvature-driven flows: a variational approach*, SIAM J. Control Optim., **31** (1993), 387-438.
[3] R. ALMGREN, *Variational algorithms and pattern formation in dendritic solidification*, J. Comput. Phys., **106** (1993), 337-354.
[4] S. ALTSCHULER - S. B. ANGENENT - Y. GIGA, *Mean curvature flow through singularities for surfaces of rotation*, J. Geom. Anal., **5** (1995), 293-358.
[5] I. ATHANASOPOULOS - L. CAFFARELLI - S. SALSA, *Degenerate phase transition problems of parabolic type. Smoothness of the front*, to appear.
[6] G. BARLES - H. M. SONER - P. E. SOUGANIDIS, *Front propagation and phase field theory*, SIAM J. Control Optim., **31** (1993), 439-469.
[7] G. BELLETTINI - M. PAOLINI, *Two examples of fattening for the curvature flow with a driving force*, Atti Accad. Naz. Lincei Cl. Sci. Fis. Mat. Natur. Rend. (9) Mat. Appl., **5** (1994), 229-236.
[8] G. BELLETTINI - M. PAOLINI, *Quasi-optimal error estimates for the mean curvature flow with a forcing term*, Diff. Integ. Eq., 8 (1995), 735-752.
[9] G. BELLETTINI - M. PAOLINI, *Some results on minimal barriers in the sense of De Giorgi applied to driven motion by mean curvature*, Rend. Accad. Naz. Sci. XL, Mem. Mat. (5), **19** (1995), 43-67.
[10] G. BELLETTINI - M. PAOLINI, *Anisotropic motion by mean curvature in the context of Finsler geometry*, Hokkaido Math. J., **25** (1996), 537-566.
[11] G. BELLETTINI - M. PAOLINI - C. VERDI, *Front-tracking and variational methods to approximate interfaces with prescribed mean curvature*, in *Numerical Methods for Free Boundary Problems* (P. NEITTAANMÄKI ed.), Birkhäuser, Basel (1991), pp. 83-92.
[12] G. BELLETTINI - M. PAOLINI - C. VERDI, *Convex approximations of functionals with curvature*, Atti Accad. Naz. Lincei Cl. Sci. Fis. Mat. Natur. Rend. (9) Mat. Appl., **2** (1991), 297-306.
[13] J. F. BLOWEY - C. M. ELLIOTT, *A phase-field model with a double obstacle potential*, in *Motion by Mean Curvature and Related Topics* (G. BUTTAZZO and A. VISINTIN eds.), Gruyter, New York, (1994), pp. 1-22.
[14] F. BREZZI - L. A. CAFFARELLI, *Convergence of the discrete free boundaries for finite element approximations*, RAIRO Modél. Math. Anal. Numér., **17** (1983), 385-395.
[15] E. BÄNSCH, *Local mesh refinement in 2 and 3 dimensions*, IMPACT Comput. Sci. Engrg., **3** (1991), 181-191.
[16] G. CAGINALP, *An analysis of a phase field model of a free boundary*, Arch. Rational Mech. Anal., **92** (1986), 205-245.
[17] X. CHEN - F. REITICH, *Local existence and uniqueness of solutions of the Stefan problem with surface tension and kinetic undercooling*, J. Math. Anal. Appl., **164** (1992), 350-362.
[18] Y. G. CHEN - Y. GIGA - S. GOTO, *Uniqueness and existence of viscosity solutions of generalized mean curvature flow equation*, J. Diff. Geom., **33** (1991), 749-786.
[19] Z. CHEN - R. H. NOCHETTO, *A posteriori error estimation for the continuous casting problem*, in preparation.
[20] Z. CHEN - R. H. NOCHETTO, *A posteriori error estimation and adaptivity for phase relaxation models*, in preparation.
[21] P. G. CIARLET, *The Finite Element Method for Elliptic Problems*, North-Holland, Amsterdam (1978).
[22] PH. CLÉMENT, *Approximation by finite element functions using local regularization*, RAIRO Modél. Math. Anal. Numér., **9** (1975), 77-84.
[23] M. G. CRANDALL - H. ISHII - P. L. LIONS, *User's guide to viscosity solutions of second order partial differential equations*, Bull. Amer. Math. Soc. (N.S.), **27** (1992), 1-67.

[24] G. Dal Maso, *An Introduction to Γ-Convergence*, Birkhäuser, Boston (1993).
[25] T. Dupont, *Mesh modification for evolution equations,* Math. Comp., **29** (1982), 85-107.
[26] G. Dziuk, *An algorithm for evolutionary surfaces,* Numer. Math., **58** (1991), 603-611.
[27] G. Dziuk, *Convergence of a semi-discrete scheme for the curvature shortening flow,* Math. Models Methods Appl. Sci., **4** (1994), 589-606.
[28] G. Dziuk, *Convergence of a semi-discrete scheme for the anisotropic curvature shortening flow*, to appear.
[29] C. M. Elliott, *Error analysis of the enthalpy method for the Stefan problem,* IMA J. Numer. Anal., **7** (1987), 61-71.
[30] C. M. Elliott - M. Paolini - R. Schätzle, *Interface estimates for the fully anisotropic Allen-Cahn equation and anisotropic mean curvature flow*, Math. Models Methods Appl. Sci., **6** (1996), 1103-1118.
[31] C. M. Elliott - R. Schätzle, *The limit of the anisotropic double-obstacle Allen-Cahn equation,* Proc. Roy. Soc. London Ser. A, to appear.
[32] C. M. Elliott - R. Schätzle, *The limit of the fully anisotropic double-obstacle Allen-Cahn equation in the non-smooth case,* SIAM J. Math. Anal., to appear.
[33] K. Eriksson - C. Johnson, *Adaptive finite element methods for parabolic problems I: a linear model problem,* SIAM J. Numer. Anal., **28** (1991), 43-77.
[34] L. C. Evans - H. M. Soner - P. E. Souganidis, *Phase transitions and generalized motion by mean curvature,* Comm. Pure Appl. Math., **45** (1992), 1097-1123.
[35] L. C. Evans - J. Spruck, *Motion of level sets by mean curvature. I,* J. Diff. Geom., **33** (1991), 635-681.
[36] F. Fierro, *Numerical approximation for the mean curvature flow with nucleation using implicit time-stepping: an adaptive algorithm,* Calcolo, to appear.
[37] F. Fierro - R. Goglione - M. Paolini, *Numerical simulations of mean curvature flow in presence of a nonconvex anisotropy,* Math. Models Methods Appl. Sci., to appear.
[38] P. C. Fife - O. Penrose, *Thermodynamically consistent models of phase-field type for the kinetics of phase transitions,* Physica D, 43 (1990), 44-62.
[39] Y. Giga - S. Goto - H. Ishii - M. H. Sato, *Comparison principle and convexity preserving properties for singular degenerate parabolic equations on unbounded domains,* Indiana Univ. Math. J., **40** (1991), 443-470.
[40] G. Huisken, *Flow by mean curvature of convex surfaces into spheres*, J. Diff. Geom., **20** (1994), 237-266.
[41] J. W. Jerome - M. E. Rose, *Error estimates for the multidimensional two-phase Stefan problem,* Math. Comp., **39** (1982), 377-414.
[42] X. Jiang - R. H. Nochetto, *A finite element method for a phase relaxation model. Part I: quasi-uniform mesh,* SIAM J. Numer. Anal., to appear.
[43] X. Jiang - R. H. Nochetto - C. Verdi, *A $P^1 - P^0$ finite element method for a model of polymer crystallization,* Comput. Meth. Appl. Mech. Engrg., **125** (1995), 303-317.
[44] X. Jiang - R. H. Nochetto - C. Verdi, *A $P^1 - P^1$ finite element method for a phase relaxation model. Part II: adaptively refined meshes,* SIAM J. Numer. Anal., to appear.
[45] M. Kimura, *Numerical analysis for moving boundary problems using the boundary tracking method,* Japan J. Indust. Appl. Math., to appear.
[46] O. W. Klein, *Existence and approximation results for phase-field systems of Penrose-Fife type and Stefan problems*, Ph.D. Thesis, Humboldt-Universität, Berlin (1997).

[47] R. KORNHUBER, *Adaptive Monotone Multigrid Methods for Nonlinear Variational Problems*, Teubner Stuttgart (1997).

[48] O. A. LADYZENSKAJA - V. SOLONNIKOV - N. URAL'CEVA, *Linear and Quasilinear Equations of Parabolic Type*, vol. TMM 23, AMS, Providence (1968).

[49] S. LUCKHAUS, *Solutions for the two-phase Stefan problem with the Gibbs-Thomson law for the melting temperature,* European J. Appl. Math., **1** (1990), 101-111.

[50] S. LUCKHAUS - T. STURZENHECKER, *Implicit time discretization for the mean curvature flow equation,* Calc. Var. Partial Differential Equations, **3** (1995), 253-271.

[51] E. MAGENES - R. H. NOCHETTO - C. VERDI, *Energy error estimates for a linear scheme to approximate nonlinear parabolic problems,* RAIRO Modél. Math. Anal. Numér., **21** (1987), 655-678.

[52] R. H. NOCHETTO, *Error estimates for multidimensional singular parabolic problems,* Japan J. Indust. Appl. Math., **4** (1987), 111-138.

[53] R. H. NOCHETTO, *A stable extrapolation method for multidimensional degenerate parabolic problems,* Math. Comp., **53** (1989), 455-470.

[54] R. H. NOCHETTO, *Finite element methods for parabolic free boundary problems*, in *Advances in Numerical Analysis*, vol. I: *Nonlinear Partial Differential Equations and Dynamical Systems* (W. LIGHT ed.), Oxford University Press, Oxford (1991), pp. 34-88.

[55] R. H. NOCHETTO - M. PAOLINI - C. VERDI, *An adaptive finite elements method for two-phase Stefan problems in two space dimensions. Part I: stability and error estimates. Supplement,* Math. Comp., **57** (1991), 73-108, S1-S11.

[56] R. H. NOCHETTO - M. PAOLINI - C. VERDI, *An adaptive finite elements method for two-phase Stefan problems in two space dimensions. Part II: implementation and numerical experiments,* SIAM J. Sci. Statist. Comput., **12** (1991), 1207-1244.

[57] R. H. NOCHETTO - M. PAOLINI - C. VERDI, *A fully discrete adaptive nonlinear Chernoff formula*, SIAM J. Numer. Anal., **30** (1993), 991-1014.

[58] R. H. NOCHETTO - M. PAOLINI - C. VERDI, *Sharp error analysis for curvature dependent evolving fronts*, Math. Models Methods Appl. Sci., **3** (1993), 711-723.

[59] R. H. NOCHETTO - M. PAOLINI - C. VERDI, *Optimal interface error estimates for the mean curvature flow*, Ann. Scuola Norm. Sup. Pisa Cl. Sci. (4), **21** (1994), 193-212.

[60] R. H. NOCHETTO - M. PAOLINI - C. VERDI, *Double obstacle formulation with variable relaxation parameter for smooth geometric front evolutions: asymptotic interface error estimates,* Asymptotic Anal., **10** (1995), 173-198.

[61] R. H. NOCHETTO - M. PAOLINI - C. VERDI, *A dynamic mesh method for curvature dependent evolving interfaces,* J. Comput. Phys., **123** (1996), 296-310.

[62] R. H. NOCHETTO - M. PAOLINI - C. VERDI, *Numerical Analysis of Geometric Motion of Fronts*, CRM, Montreal, in preparation.

[63] R. H. NOCHETTO - A. SCHMIDT - C. VERDI, *A posteriori error estimation and adaptivity for degenerate parabolic problems,* Math. Comp., to appear.

[64] R. H. NOCHETTO - A. SCHMIDT - C. VERDI, *Mesh and time step modification for degenerate parabolic problems*, in preparation.

[65] R. H. NOCHETTO - A. SCHMIDT - C. VERDI, *Adaptive algorithm and simulations for Stefan problems in two and three dimensions,* in preparation.

[66] R. H. NOCHETTO - A. SCHMIDT - C. VERDI, *Adapting meshes and time-steps for phase change problems*, Atti Accad. Naz. Lincei Cl. Sci. Fis. Mat. Natur. Rend. (9) Mat. Appl., to appear.

[67] R. H. NOCHETTO - C. VERDI, *Approximation of degenerate parabolic problems using numerical integration,* SIAM J. Numer. Anal., **25** (1988), 784-814.

[68] R. H. NOCHETTO - C. VERDI, *An efficient linear scheme to approximate parabolic free boundary problems: error estimates and implementation,* Math. Comp., **51** (1988), 27-53.
[69] R. H. NOCHETTO - C. VERDI, *Convergence of double obstacle problems to the generalized geometric motion of fronts,* SIAM J. Math. Anal., **26** (1995), 1514-1526.
[70] R. H. NOCHETTO - C. VERDI, *Approximating curvature driven interfaces with applications to shape recovery,* in *Curvature Flows and Related Topics* (A. DAMLAMIAN *et al.*, eds.), Gakkötosho, Tokyo (1995), pp. 159-177.
[71] R. H. NOCHETTO - C. VERDI, *Combined effect of explicit time-stepping and quadrature for curvature driven flows,* Numer. Math., **74** (1996), 105-136
[72] R. H. NOCHETTO - C. VERDI, *Convergence past singularities for a fully discrete approximation of curvature driven interfaces,* SIAM J. Numer. Anal., **34** (1997), 490-512.
[73] S. OSHER - J. A. SETHIAN, *Fronts propagating with curvature dependent speed: algorithms based on Hamilton-Jacobi formulations,* J. Comput. Phys., **79** (1988), 12-49.
[74] M. PAOLINI, *An efficient algorithm for computing anisotropic evolution by mean curvature,* in *Curvature Flows and Related Topics* (A. DAMLAMIAN *et al.* eds.), Gakkötosho, Tokyo (1995), pp. 119-213.
[75] M. PAOLINI - C. VERDI, *Asymptotic and numerical analyses of the mean curvature flow with a space-dependent relaxation parameter,* Asymptotic Anal., **5** (1992), 553-574.
[76] J. RULLA - N. J. WALKINGTON, *Optimal rates of convergence for degenerate parabolic problems in two dimensions,* SIAM J. Numer. Anal., **33** (1996), 56-67.
[77] A. SCHMIDT, *Computation of three dimensional dendrites with finite elements,* J. Comput. Phys., **125** (1996), 293-312.
[78] J. A. SETHIAN, *Level Set Methods*, Cambridge University Press, Cambridge (1996).
[79] C. VERDI, *Optimal error estimates for an approximation of degenerate parabolic problems,* Numer. Funct. Anal. Optim., **9** (1987), 657-670.
[80] C. VERDI, *Numerical aspects of parabolic free boundary and hysteresis problems,* in *Phase Transition and Hysteresis* (A. VISINTIN ed.), Lectures Notes in Mathematics, 1584, Springer-Verlag, Berlin (1994), pp. 213-284.
[81] C. VERDI - A. VISINTIN, *Error estimates for a semiexplicit numerical scheme for Stefan-type problems,* Numer. Math., **52** (1988), 165-185.
[82] A. VISINTIN, *Stefan problem with phase relaxation,* IMA J. Appl. Math., **34** (1985), 225-245.
[83] A. VISINTIN, *Models of Phase Transitions*, Birkhäuser, Boston (1996).
[84] A. VISINTIN, *Nucleation and mean curvature flow,* Comm. Partial Differential Equations, to appear.
[85] A. VISINTIN, *Introduction to the models of phase transitions*, this volume, p. 1.

Dipartimento di Matematica, Università di Milano
Via Saldini 50, 20133 Milano, Italy
e-mail address: verdi@paola.mat.unimi.it

Pervenuta in Redazione
il 22 settembre 1997